Methods to Estimate Respiratory Rate Using the Photoplethysmography Signal

Ayalon Angelo de Moraes Filho[a], Guilherme Schreiber[b], Julio Alexander Sieg[c], Maicon Diogo Much[d], Vanessa de Moura Bartoski[e] and César Marcon[f]
School of Technology, Pontifical Catholic University of Rio Grande do Sul, Porto Alegre, Brazil

Keywords: Health, Photoplethysmography, Respiratory Rate Estimation.

Abstract: Academia and industry have devoted significant effort to the research and development of smart wearable devices applied to health monitoring. The photoplethysmography (PPG) sensor is widely used for monitoring biosignals, such as heart and respiratory rate (RR), which are influenced by the cardiovascular system. This work focuses on analyzing methods for RR estimation regarding the effect of breathing on the PPG signal variation. This work describes, implements, and analyzes four methods for estimating RR. These methods are based on capturing RR using Fast Fourier Transform, median, and extracting physiological characteristics induced by respiration in the PPG signal. The most efficient method merges three RR calculations analyzed on the same signal, achieving nearly 93% of efficacy in the best scenario. The method efficacies were calculated using PPG signals from the BIDMC and CapnoBase databases collected from patients during hospital care. The analysis allows for understanding and mitigating the RR estimation challenges and evaluating the most efficacy method for a wearable device monitoring scenario.

1 INTRODUCTION

The aging population, the availability of mobile broadband connectivity, and the development of sophisticated technologies have driven the adoption of personalized, digital, or remote patient monitoring methods. This process was further accelerated with the emergence of the coronavirus pandemic, which increased pressure on limited hospital facilities, requiring medical service providers to accelerate the research and implementation of new technologies for monitoring health outside the hospital (Olivadoti, 2022), especially in the patient's home.

Sensor innovations allow vital signs to be measured with clinical-grade accuracy in a residential setting. Wearable devices are more accessible, enabling home monitoring of philological signs, such as body temperature, heart rate, Respiratory Rate (RR), blood pressure, and oxygen saturation.

RR is a valuable diagnostic and prognostic marker of health. In hospital healthcare, it is a highly sensitive marker of acute deterioration. For example, an elevated RR predicts cardiac arrest and in-hospital mortality and may indicate respiratory dysfunction. Consequently, RR is measured between four and six hours in hospitalized patients with acute illness. RR is also used in emergency triage. In primary care, RF is used to identify pneumonia and as a marker of pulmonary embolism. However, RR is usually measured by manually counting chest wall movements (outside intensive care) and is a time-consuming, imprecise, and poorly performed process (Charlton et al., 2018).

The optical photoplethysmograph (PPG) sensor is commonly found among wearable physiological signal monitoring devices, such as pulse oximeters, due to its simplicity, low cost, and non-invasive approach. The PPG sensor is directly related to the cardiovascular system, detecting blood content and volume changes in the microvascular system. Because the cardiovascular and respiratory systems are correlated, researchers have made efforts to develop algorithms capable of inferring the respiration rate from the PPG signal.

[a] https://orcid.org/0000-0001-7044-1504
[b] https://orcid.org/0000-0002-1037-4853
[c] https://orcid.org/0000-0003-3966-9855
[d] https://orcid.org/0000-0002-1760-907X
[e] https://orcid.org/0000-0001-6365-9273
[f] https://orcid.org/0000-0002-7811-7896

Moraes Filho, A., Schreiber, G., Sieg, J., Much, M., Bartoski, V. and Marcon, C.
Methods to Estimate Respiratory Rate Using the Photoplethysmography Signal.
DOI: 10.5220/0011729100003414
In *Proceedings of the 16th International Joint Conference on Biomedical Engineering Systems and Technologies (BIOSTEC 2023) - Volume 5: HEALTHINF*, pages 445-452
ISBN: 978-989-758-631-6; ISSN: 2184-4305

The main objective of this work is to present RR inference methods from PPG signals for obtaining the best efficiency for absolute error equal to 0 breaths per minute (rpm) in the analyzed data.

2 THEORETICAL FOUNDATION

PPG is used to measure blood volume changes in the microvascular tissue bed under the skin; these changes occur due to the pulsatile nature of the circulatory system (Kamal et al., 1989). As an optical technique, PPG requires a light source and a photodetector. Light passing through biological tissue can be absorbed by different substances, including pigments in skin, bones, and arterial and venous blood. Most changes in blood flow occur primarily in the arteries and arterioles. PPG sensors optically detect changes in blood flow volume (i.e., changes in detected light intensity) in the microvascular tissue bed, either through reflection or transmission through the tissue (Tamura et al., 2014).

Figure 1 exemplifies a PPG waveform consisting of direct current (DC) and alternating current (AC) components. The DC component corresponds to the transmitted or reflected optical signal detected in the tissue; this component depends on the tissue structure and the average volume of arterial and venous blood. The AC component shows changes in blood volume between the cardiac cycle's systolic and diastolic phases; the AC component's fundamental frequency depends on the heart rate and is superimposed on the DC component (Tamura et al., 2014).

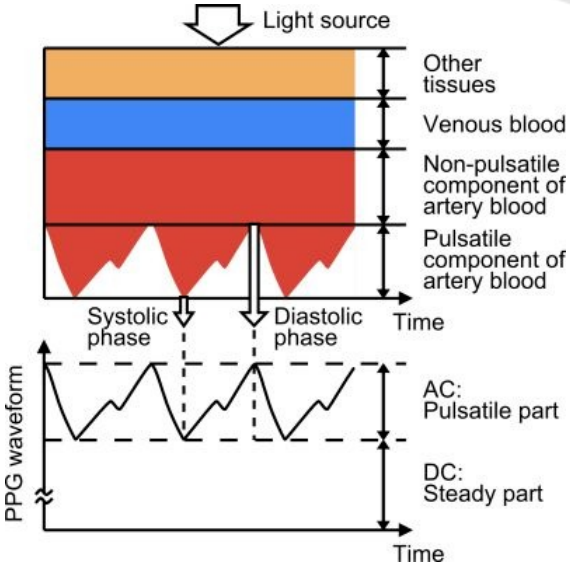

Figure 1: PPG waveform example (Tamura et al., 2014).

PPG pulse wave morphology is influenced by (i) the heart, which considers cardiac ejection characteristics, including heart rate and rhythm, and stroke volume; (ii) circulation, including cardiovascular properties such as arterial stiffness and blood pressure; (iii) additional physiological processes, including breathing and the autonomic nervous system, that can be affected by stress; and (iv) diseases (Mejıa-Mejıa et al., 2021). The quality of the PPG signal depends on the wavelength of the light, measurement location, i.e., sensor attachment location, contact force, motion artifacts, the breathing of the individual being measured, and ambient temperature (Tamura & Maeda, 2018). These factors generate various types of additive noise (artifacts) that can be contained in PPG signals, affecting signal characteristics.

Respiratory-induced changes in intrathoracic pressure are transmitted to the central veins, generating a change in blood pressure that the spectrum of the PPG signal can detect. Breathing can induce variations in the PPG signal in three ways (Dehkordi, 2018):

- Respiratory-Induced Intensity Variation (***RIIV***) - Changes in venous return due to changes in intrathoracic pressure throughout the respiratory cycle cause a modulation of the baseline (i.e., the continuous component - DC) of the PPG signal;
- Respiratory-Induced Amplitude Variation (***RIAV***) - During inspiration, the systolic volume of the left ventricle decreases due to changes in intrathoracic pressure, reducing the pulse amplitude and the opposite happens during expiration;
- Respiratory-Induced Heart Rate Variation (***RIFV***) - Heart rate varies throughout the respiratory cycle, increasing during inspiration and decreasing during expiration.

3 RELATED WORK

Table 1 stands 19 works and the one proposed here concerning (i) the year of publication, (ii) the foundation that guides the extraction of the RR, (iii) the extraction method used, (iv) the domain in which the signals were analyzed; and (v) database used to obtain the PPG signal.

The Base column of Table 1 shows that the RR extraction from most works is based on the physiological characteristics of breathing, with a smaller portion of the works employing the PPG signal filtering process. When we analyze the filtering methods in isolation, represented by ***Fl***, we realize

Table 1: Related work comparison.

Article	Base	Method	Domain	Dataset
Pimentel et al., 2017	Rpc	FFT*, RIIV, RIAV, RIFV, Fusion	Freq.	CapnoBase, BIDMC
Orphanidou, 2017	Rpc	EEMD, RIAV, RIFV	Tempo	Ad hoc
Motin et al., 2018	Fl	FFT, EEMD	Freq.	CapnoBase, MIMIC
Khreis et al., 2018	Rpc	RIIV, RIAV, RIFV	Time	CapnoBase
Birrenkott et al., 2018	Rpc	FFT*, RIIV, RIAV, RIFV	Freq.	CapnoBase, MIMIC
Motin et al., 2019	Fl	EMD, EEMD, CEEMD, CEEMDAN, ICEEMDAN	Time	CapnoBase, MIMIC
Yang, 2019	Rpc	FFT*, RIIV, RIAV, RIFV, Fusion	Freq.	Ad hoc
Pollreisz and Nejad, 2020	Rpc	FFT*, RIIV, RIAV, RIFV, Fusion	Freq.	Ad hoc
Motin et al., 2020	Fl	FFT*, EEMD, RIIV, RIAV, RIFV	Freq.	Ad hoc
Pollreisz and TaheriNejad, 2020	Rpc	FFT*, RIFV	Freq.	Ad hoc
Khreis et al., 2020	Rpc	FFT*, RIIV, RIAV, RIFV	Freq.	CapnoBase, Sherpam
Lazazzera and Carrault, 2020	Fl, Rpc	FFT*, EMD, DWT, RIIV, RIAV, RIFV, Fusion	Freq.	CapnoBase
Kozumplik et al., 2021	Rpc	FFT*, RIIV, RIAV	Freq., Time	CapnoBase, BIDMC
Fikriastuti and Muhaimin, 2021	Rpc	FFT, RIIV, RIAV, RIFV, Fusion	Freq.	CapnoBase
Protopsaltis et al., 2021	Rpc	FFT*, RIIV, RIAV, RIFV, Fusion	Freq.	CapnoBase, Ad hoc
Haddad et al., 2021	Rpc	RIIV, RIAV, RIFV, Fusion	Time	CapnoBase
Icazatti et al., 2021	Fl	FIR	Time	BIDMC, CCSHS
Adami et al., 2021	Fl	FFT*, EMD, DWT	Freq.	BIDMC, MIT-BIH
Chen et al. 2021	Rpc	FFT*, RIIV, RIAV, RIFV, Fusion	Freq.	Ad hoc
This work	Fl, Rpc	FFR*, Median, RIIV, Fusion	Freq., Time	BIDMC, CapnoBase

LEGEND: ***Rpc*** – Respiratory physiological characteristics; ***Fl*** – Only applying Filters
Freq. – Frequency domain; ***Time*** – Time domain
FFT – Fast Fourier Transform; ***FFT**** – FFT used to extract the spectral frequency without capturing RR directly
RIIV, ***RIAV***, ***RIFV*** – Respiratory-Induced Variation regarding Intensity, Amplitude and Frequency, respectively
Fusion – extract RR correlating RIIV, RIAV, RIFV; ***EMD*** – Empirical Mode Decomposition
EEMD, ***CEEMD***, ***CEEMDAN***, ***ICEEMDAN*** – Special methods based on EMD
DWT – Discrete Wavelet Transform; ***Median*** – extracts RR from the baseline variation of the PPG signal median

that most of the works (Motin et al., 2018) (Motin et al., 2019) (Motin et al., 2020) (Lazazzera and Carrault, 2020) (Adami et al., 2021) extracts RR using EMD and its variations (see column Method).

We identified the predominance of RIIV, RIAV, and RIFV modulations in the analysis referring to the extraction of RR based on respiratory physiological characteristics, represented by ***Rpc*** in the Base column.

Additionally, we divided the articles that extract the RR based on the physiological characteristics of breathing into three sets. These sets are composed of works that assess the performance of RIIV, RIAV, and RIIF: (i) only individually (Pollreisz and TaheriNejad, 2020) (Lazazzera and Carrault, 2020) (Kozumplik et al., 2021); (ii) individually, but consider RR obtained with the highest quality index (Khreis et al., 2018)(Birrenkott et al., 2018)(Khreis et al., 2020); (iii) merging the partial RR values obtained in each modulation to calculate the final RR (Pimentel et al., 2017) (Orphanidou, 2017) (Yang, 2019) (Pollreisz and Nejad, 2020) (Lazazzera and Carrault, 2020) (Fikriastuti, and Muhaimin, 2021) (Protopsaltis et al., 2021) (Haddad et al., 2021) (Chen et al., 2021).

The Domain column points out that most of the works estimate RR by analyzing the signals in the frequency domain, except for (Orphanidou, 2017) (Khreis et al., 2018) (Motin et al., 2019) (Haddad et al., 2021) (Icazatti et al., 2021) that employ the time domain. Consequently, we explored the RR extraction with methods that analyze both the time and frequency domains, and we chose to employ the Fast Fourier Transform (FFT) in all implemented methods.

The Database column shows that most works use CapnoBase, followed by the MIMIC and BIDMC databases. This reason led us to choose the CapnoBase and BIDMC databases in this work, which are freely available and organized to obtain RR from the PPG signal analysis. Additionally, we decided to include the Synthetic Dataset from the

Respiratory Rate Estimation project (Charlton, 2016) to assess the ideal measurement time window, given that data is in a noise-free environment.

The work proposed here developed three algorithms entitled “FFT Method”, “Median Method”, and “RIIV Method” to study the performance when extracting the respiratory rate in signals containing respiration-induced baseline modulation. Besides, the work proposed here implements the “Fusion Method”, which in its initial stage evaluates RRs obtained with the three baseline methods and merges these values when a given criterion is accepted; otherwise, the measurement is discarded.

4 METHODS FOR ESTIMATING RESPIRATORY RATE

We implemented four methods to analyze the effectiveness and efficiency of RR estimations from the PPG signal. These methods enable estimating RR (i) using an FFT; (ii) Median; (iii) exploring breath-induced intensity variations, i.e., RIIV; and (iv) integrating multiple RR estimates.

4.1 Fast Fourier Transform Method

The Fast Fourier Transform (FFT) quickly calculates the discrete Fourier transform of a data sequence, allowing us to obtain the signal frequency spectrum. FFT is one of the most used methods to analyze signals in the frequency domain because time is mathematically eliminated during the transformation process, resulting only in signal frequency components (Tamura and Maeda, 2018).

This method uses the SciPyfft function of the Python SciPy library to return the discrete Fourier transform of a real or complex sequence (Bluestein, 1970). The extraction of RR from the PPG signal follows the following steps:

- Converting the PPG signal from the time domain to the frequency domain applying FFT;
- Transforming the frequency value to “rpm” by multiplying the dominant peak value by 60;
- Identifying the dominant frequencies by extracting the RR value within the acceptable range for humans - between 4 rpm (0.06 Hz) and 60 rpm (1 Hz).

4.2 Median Method

The Median Filter allows extracting the baseline present in the PPG signal (Awodeyi et al., 2013). The Median Method explores the baseline variation by calculating the PPG signal median.

This method uses the numpy.median function of the Python Numpy library to return the median of the vector elements. The RR extraction from the PPG signal requires the following steps:

- Calculating the median with a sliding vector of the signal sample rate size;
- Applying the FFT in the resulting vector and selecting the dominant frequency peak within the valid RR range;
- Multiplying the dominant frequencies by 60 to convert to “rpm”.

4.3 RIIV Method

The RIIV Method explores baseline variations obtained through linear interpolation between the PPG signal peaks. We implemented this method using the SciPy.find_peaks and SciPy.interpolate, present in the Python SciPy library, which returns a vector containing all the peaks of a signal and function whose calling method interpolates to find the value of new points (Bluestein, 1970).

RR can be acquired with an analysis in time or frequency. Time analysis is achieved by counting peaks or valleys in the signal. Frequency analysis requires the FFT application; in this case, RR is the dominant signal frequency generated by the FFT within the RR human spectrum. The RR measured by the respiration-induced variation methods is performed via the following steps:

- Extraction of the induced baseline variation in the PPG signal to get the respiratory signal in time;
- FFT Application on the respiratory signal and selection of the dominant frequency peak within the valid RR spectrum;
- Multiplying the dominant frequencies by 60 to convert to “rpm”.

4.4 Fusion Method

Merging RR estimates complements the three methods discussed earlier. This method ascends the RR values obtained by the FFT, Median, and RIIV methods, creating a three-position vector containing the smallest (min), intermediate (itr), and largest (max) values, and considers an error (ε) between these values to determine the merge rule.

The determination of the error value is empirical, and for this work, ε=0 rpm was chosen to perform an in-depth analysis of the results.

The RR fusion estimate is constructed using the

following conditions and considering their ordering:

- If the difference between the smallest and largest vector value is less than or equal to the error, then RR is the average of the three values. The reason is to assume that if the three samples are close, then they must be close to the true RR value;
- If the above conditions are not satisfied, RR is not measured. As there is no consensus on the best estimate, the method characterizes the sample as a noisy signal, and the estimated value is discarded. RR cannot be measured in an extreme situation where this condition occurs in all samples.

$$RR = \begin{cases} \frac{min + itr + max}{3} & \text{if } |min - max| \leq \varepsilon \\ \text{not evaluated} & \text{otherwise} \end{cases}$$

5 EXPERIMENTAL RESULTS – SYNTHETIC DATA

Synthetic Dataset is a database created in the Respiratory Rate Estimation project that contains synthetic ECG and PPG signals (Charlton, 2016). These signals were developed to verify the performance of methods to estimate RR in a scenario without external noise. The dataset includes PPG signals in the RR range between 4 and 60 rpm, modulated in isolation concerning baseline, amplitude, and frequency. It contains mathematically equated PPG signals, not including external interferences during its construction, enabling to get accurate information on the influence of the window size used for the RR measurement.

The initial length of the observation window was empirically selected to be equal to 10s. Note that a huge observation window requires a long time to obtain a sample value; however, a tiny observation window can lead to inaccuracy. The initial value was considered the "smallest observation window" to measure the RR. Subsequently, a value equivalent to "smallest window" was added to find an observation window size in which the absolute error between the reference value and the estimated value remained unchanged. This is considered the minimum precision window; upper observation windows should not change the RR results due to data subsampling.

All the methods analyzed in this section presented stable values with an absolute error equal to zero for observation windows greater than 50s. The observation window of 10s was the only one that presented an absolute error equal to 2 rpm, being considered the highest error found. The window of 30s presented an absolute error equal to zero.

Some estimates obtained with 40s windows were worse than the 30s estimates due to the signal being synthetic, so the multiplicity of 40s generates a precision error for the 500Hz samples. This finding was essential to understand the influence of the sampling rate in obtaining the best observation window. Additionally, this finding indicates that it is impossible to define an optimal observation window value because it depends on the PPG signal.

6 EXPERIMENTAL RESULTS – REAL DATA

The CapnoBase dataset (Karlen, 2010) contains ECG, pulse oximetry with PPG, and CO_2 data from 42 cases, each described by an 8min recording. In addition, CapnoBase provides the RR measured for everyone, enabling us to evaluate the methods used.

BIDMC (Pimentel et al., 2018) is a dataset used to assess the performance of RR methods. BIDMC contains information from ECG, PPG pulse oximetry, and respiratory signs from impedance pneumography. All these signals were acquired from 53 intensive care patients, with recordings lasting 8min for each patient.

Figure 2 presents the configurations performed to obtain the experimental data. The CapnoBase and BIDMC databases underwent an equalization process to obtain consistent RF reference values throughout the sampling interval. The equalization generated the banks called CapnoBase* and BIDMC*, which contain sensory data from 42 and 53 people, respectively; this data corresponds to 95 PPG signals, each with 360s of sampling.

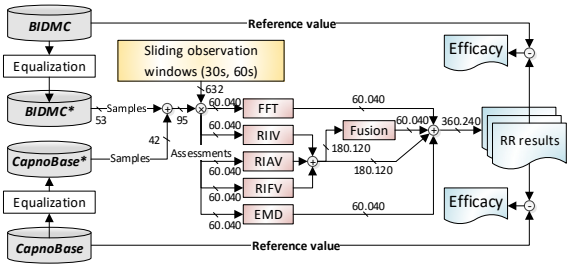

Figure 2: Settings performed to obtain experimental data.

These samples were evaluated by the FFT, Median, RIIV, and Fusion methods in sliding observation windows of 30s and 60s to assess estimation errors with different window sizes.

Additionally, we chose to use sliding windows with a base of 1s to smooth the passage from one

sample to another – this approach was also adopted by Fikriastuti and Muhaimin (2021). Using a sliding window of 1s, within the range of 360s, implied 331 and 301 samples for the observation windows of 30s and 60s, respectively. We chose to work with only six minutes (360s) of the databases containing eight-minute samples, removing the initial and final minutes of each patient; this choice was made empirically to remove the edges of the databases and eliminate possible erroneous measurements.

This procedure results in 632 observation windows for each of the 95 PPG signals; consequently, 60,040 evaluations must be carried out using three of the four proposed methods – except for the Fusion Method, which takes the results of the FFT, Median, and RIIV methods as input. The execution of all experiments results in 360,240 RR estimates, whose absolute error and corresponding effectiveness are evaluated by comparing with the reference values included in the CapnoBase and BIDMC databases.

The Fusion Method evaluates the quality of the signal when it integrates the three RR values obtained—performing this method on CapnoBase data removed 5722 and 4949 samples for observation windows of 30s and 60s, respectively. Similarly, BIDMC had 7493 and 6745 samples removed for observation windows of 30s and 60s, respectively. This removal is not directly related to the noise in the database but instead to the discrepancy between the FFT, Median, and RIIV methods, which did not allow the Fusion Method to choose the best estimate to be taken. Because of these removals, all the percentage analyses presented in this section subtract the samples classified as noisy from the total amount of samples for the Fusion Method.

The two databases contain the reference RRs for each PPG signal. However, in some cases, the reference values to assess the CapnoBase RR were only present in the range of 7s to 72s or smaller intervals. In comparison, each patient has a total of 480s (8min) to store the PPG signal and its respective respiratory reference signal (CO_2). To obtain the RR reference values over the entire 360s interval explored in the database, we applied an FFT on the CO_2 signal.

To maintain similarity in the analysis of the two databases, we applied the same procedure to the Impedance signal present in the BIDMC database. This process in both databases was called Equalization. However, the Equalization approach can fail when the analyzed window contains noise that overlaps the respiratory signal, as illustrated in Figure 3. Since the respiratory signal is not evaluated correctly, the RR estimates will likely suffer deviations that can alter the efficacy analysis of the evaluated methods.

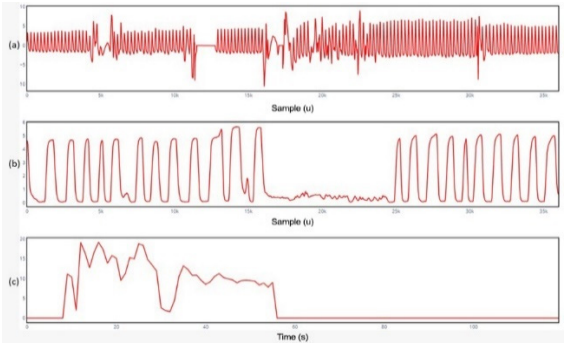

Figure 3: Example of CapnoBase data containing intense noise that overlaps with (a) PPG and (b) CO_2 signal, and (c) RR reference values.

We decided to evaluate two window observation sizes (30s and 60s), as the variability contained in the databases can generate artifacts that can be minimized in larger windows. Finally, we chose to work with only 6 minutes of the databases containing eight-minute samples, discarding the initial and final minutes of each patient. Figure shows the percentage of samples with 100% accuracy in the RR obtained with each evaluated method, considering the data provided by CapnoBase and BIDMC for both observation windows. Regarding only the CapnoBase dataset, the result analysis shows an average variation of practically 5% error with the observation window reduction. This variation indicates that the proposed methods improve the RR estimates as the observation window increases. Additionally, the Fusion Method obtains the highest efficacy, improving the quality of the estimates obtained with the other methods.

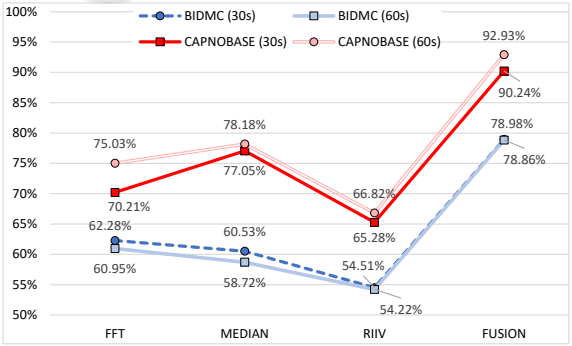

Figure 4: Percentage of samples reaching 100% efficacy using CapnoBase and BIDMC datasets and sliding observation windows of 30s and 60s.

The results of BIDMC indicate many similarities in the data contained in the databases. Clear examples

are the Fusion Method, which had the best results for the BIDMC and CapnoBase databases, and the RIIV method, which had the lowest estimates in both databases. Additionally, the 60s observation window performed poorly compared to the results obtained with 30s windows.

Figure presents the same experiment as Figure but highlights the number of RR samples that had errors of 3 rpm or more. Once again, it is possible to observe that the Fusion Method achieves the best results for both databases and observation windows, with the worst results obtained with the RIIV Method. Although RR estimates with errors of 3 rpm or more may be unacceptable, the number of samples with these values is proportionally low when using Fusion Method. Additionally, samples with high errors are interlaced with samples of greater efficacy, enabling filtering software to remove sudden variations between samples and improving the average accuracy of the RR estimate.

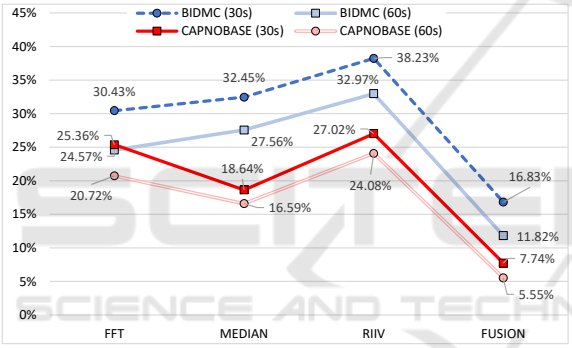

Figure 5: Percentage of samples with errors upper to 3 rpm of RR using CapnoBase and BIDMC datasets and sliding observation windows of 30s and 60s.

Additionally, Figure and Figure display that all methods are more effective when working with the CapnoBase database, and Fusion and RIIV methods have the best and worst performances among the methods, respectively. However, the same efficacy was not achieved with the BIDMC database. A possible reason for this achievement is acquired when visually analyzing the PPG signals; i.e., a higher number of samples with artifacts was identified in the BIDMC database, which is the main reason for the methods having lower performance compared to the evaluations made with CapnoBase.

7 CONCLUSION

This work evaluated the effectiveness of four methods for inferring the respiratory rate of PPG signals available in synthetic databases. The Fusion Method showed the highest efficiency among the evaluated methods, mainly because the merger achieved, on average, the best results of the correlated methods. The proposed methods can be easily implemented within firmware on a wearable device, making it possible to evaluate the methods explored in this work in real scenarios and in real-time. As a future work, we intend to compare the methods proposed here with other works described in the literature to assess the relative effectiveness of the approaches.

ACKNOWLEDGMENT

This study was financed in part by the Coordination for the Improvement of Higher Education Personnel - Brazil (CAPES) - Finance Code 001, National Council for Scientific and Technological Development (CNPq) and Financier of Studies and Projects (FINEP).

REFERENCES

Olivadoti, G. (2022). How Advances in Sensor and Digital Technology Yield Better Patient Care, *Thought Leadership Article, Analog Devices*, pp. 1-2.

Charlton, P., Birrenkott, D., Bonnici, T., Pimentel, M., Johnson, A., Alastruey, J., Tarassenko, L., Watkinson, P., Beale, R., Clifton, D. (2018). Breathing Rate Estimation from the Electrocardiogram and Photoplethysmogram: A Review, *IEEE Reviews in Biomedical Engineering*, v. 11, pp. 2-20.

Karlen, W., Turner, M., Cooke, E., Dumont, G., Ansermino, J., (2010). CapnoBase: Signal database and tools to collect, share and annotate respiratory signals, *Proceedings of the Annual Meeting of the Society for Technology in Anesthesia (STA)*, pp. 1-27.

Pimentel, M., Johnson, A., Charlton, P., Clifton, D. (2018). BIDMC PPG and Respiration Dataset, *https://physionet.org/content/bidmc/1.0.0/*.

Kamal, A., Harness, J., Irving, G., Mearns, A. (1989). Skin photoplethysmography—a review, *Computer methods and programs in biomedicine, v. 28, n. 4, pp. 257-269*.

Tamura, T., Maeda, Y., Sekine, M., Yoshida, M. (2014). Wearable photoplethysmographic sensors—past and present, *Electronics, v. 3, n. 2, pp. 282-302*.

Mejıa-Mejıa, E., Allen, J., Budidha, K., El-Hajj, C., Kyriacou, P., Charlton, P. (2021). Photoplethysmography Signal Processing and Synthesis", *Photoplethysmography - Technology, Signal Analysis and Applications, Academic Press, chap. 4, pp. 69-146*.

Tamura, T. and Maeda, Y. (2018) Pulse and Flow – Photoplethysmogram, *Seamless Healthcare Monitoring - Advancements in Wearable, Attachable, and Invisible Devices, Springer, Part III, pp. 159-192*.

Dehkordi, P., Garde, A., Molavi, B., Ansermino, J., Dumon, G. (2018). Extracting Instantaneous Respiratory Rate from Multiple Photoplethysmogram Respiratory-Induced Variations, *Frontiers in Physiology, v. 9, pp. 948.1-948.10*.

Charlton, P., Bonnici, T., Tarassenko, L., Clifton, D., Beale, R., Watkinson, P. (2016). An Assessment of Algorithms to Estimate Respiratory Rate from The Electrocardiogram and Photoplethysmogram, *Physiological Measurement, v. 37, n. 4, pp. 610-626*.

Pimentel, M., Johnson, A., Charlton, P., Birrenkott, D., Watkinson, P., Tarassenko, L. Clifton, D. (2017). Toward a Robust Estimation of Respiratory Rate from Pulse Oximeters, *IEEE Transactions on Biomedical Engineering, v. 64, n. 8, pp. 1914-1923.*

Orphanidou, C. (2017). Derivation of respiration rate from ambulatory ECG and PPG using Ensemble Empirical Mode Decomposition: Comparison and fusion, *Computers in Biology and Medicine, v. 81, pp. 45-54*.

Motin, M., Karmakar, C. Palaniswami, M. (2018) Ensemble Empirical Mode Decomposition with Principal Component Analysis: A Novel Approach for Extracting Respiratory Rate and Heart Rate from Photoplethysmographic Signal, *IEEE Journal of Biomedical and Health Informatics, v. 22, n. 3, pp. 766-774*.

Khreis, S., Ge, D., Carrault, G. (2018). Estimation of Breathing Rate from the Photoplethysmography Using Respiratory Quality Indexes, *Proceedings of the Computing in Cardiology Conference (CinC), pp. 1-4*.

Birrenkott, D., Pimentel, M., Watkinson, P., Clifton, D. (2018). A Robust Fusion Model for Estimating Respiratory Rate from Photoplethysmography and Electrocardiography, *IEEE Transactions on Biomedical Engineering, v. 65, n. 9, pp. 2033-2041*.

Motin, M., Karmakar, C., Palaniswami. M. (2019). Selection of Empirical Mode Decomposition Techniques for Extracting Breathing Rate From PPG, *IEEE Signal Processing Letters, v. 26, n. 4, pp. 592-596.*

Yang, H., Li, M., He, D., Che, X., Qin, X. (2019). Respiratory Rate Estimation from the Photoplethysmogram Combining Multiple Respiratory-induced Variations Based on SQI, *Proceedings of the IEEE International Conference on Mechatronics and Automation (ICMA), pp. 382-387.*

Pollreisz D. and Nejad, N. (2020). Reliable Respiratory Rate Extraction using PPG, *Proceedings of the IEEE Latin American Symposium on Circuits & Systems (LASCAS), pp. 1-4*.

Motin, M., Karmakar, C., Kumar, D., Palaniswami, M., (2020). PPG Derived Respiratory Rate Estimation in Daily living Conditions, *Proceedings of the Annual International Conference of the IEEE Engineering in Medicine & Biology Society (EMBC), pp. 2736-2739*.

Pollreisz, D. and TaheriNejad, N. (2020). Efficient Respiratory Rate Extraction on a Smartwatch, *Proceedings of the Annual International Conference of the IEEE Engineering in Medicine & Biology Society (EMBC), pp. 5988-5991*.

Khreis, S., Ge, D., Rahman, H., Carrault, G. (2020). Breathing Rate Estimation Using Kalman Smoother with Electrocardiogram and Photoplethysmogram, *IEEE Transactions on Biomedical Engineering, v. 67, n. 3, pp. 893-904.*

Lazazzera, R. and Carrault, G. (2020). Breathing Rate Estimation Methods from PPG Signals, on CapnoBase Database, *Proceedings of the Computing in Cardiology (CinC), v. 47, pp. 1-4.*

Kozumplik, J., Smital, L., Nemcova, A., Ronzhina, M., Smisek, R., Marsanova, L., Kralik, M., Vitek, M. (2021). Respiratory Rate Estimation Using the Photoplethysmogram: Towards the Implementation in Wearables, *Proceedings of the Computing in Cardiology (CinC), v. 48, pp. 1-4*.

Fikriastuti, N. and Muhaimin, H. (2021). Respiratory Rate Estimations using Three Respiratory-Induced Variations on Photoplethysmogram, *Proceedings of the International Conference on Electrical Engineering and Informatics (ICEEI), pp. 1-6*.

Protopsaltis, G., Krizea, M., Gialelis, J. (2021). Continuous Measurement of Respiratory Rate via Single-Wavelength Reflective Photoplethysmography, *Proceedings of the Mediterranean Conference on Embedded Computing (MECO), pp. 1-5.*

Haddad, S., Boukhayma, A., Caizzone, A. (2021). PPG-Based Respiratory Rate Monitoring Using Hybrid Vote-Aggregate Fusion Technique, *Proceedings of the Annual International Conference of the IEEE Engineering in Medicine & Biology Society (EMBC), pp. 1605-1608*.

Icazatti, F., Dell'Aquila, C., Leber, E. (2021). Design and validation of a respiratory rate estimation algorithm based on photoplethysmography (PPG) signal, *Proceedings of the Workshop on Information Processing and Control (RPIC), pp. 1-5*.

Adami, A., Boostani, R., Marzbanrad, F., Charlton, P. (2021). A New Framework to Estimate Breathing Rate from Electrocardiogram, Photoplethysmogram, and Blood Pressure Signals, *IEEE Access, v. 9, pp. 45832-45844*.

Chen, M., Zhu, Q., Wu, M. and Wang, Q. (2021). Modulation Model of the Photoplethysmography Signal for Vital Sign Extraction, *IEEE Journal of Biomedical and Health Informatics, v. 25, n. 4, pp. 969-977.*

Bluestein, L. (1970). A linear filtering approach to the computation of discrete Fourier transform. *IEEE Transactions on Audio and Electroacoustics, v. 18, n. 4, pp. 451-455*.

Awodeyi, A., Alty, S. and Ghavami, M. (2013). Median Filter Approach for Removal of Baseline Wander in Photoplethysmography Signals, *European Modelling Symposium, pp. 261-264.*